Synthesis, Characterization and Comparative studies of Lithium Doped $NiFe_2O_4$ Thin Films by SILAR Method for Supercapacitor Application

V. S. Jamadade[1*], P. K. Pagare[2], Dhanshri S. Gaikwad[1], A. S. Burungale[3], V. S. Sawant[1]

[1]Department of Physics, D. P. Bhosale College Koregaon, Satara, Maharashtra-415501, India
[2]Dr. A. P. J. Abdul Kalam Research Laboratory, Department of Physics, Yashavantrao Chavan Institute of Science, Satara, Maharashtra-415001, India
[3]Department of Chemistry, S.M. Joshi College, Hadpsar, Pune, Maharashtra 411028, India

Abstract:

Lithium doped and undoped $NiFe_2O_4$ thin films have been successfully deposited onto stainless steel substrates using cost-effective successive ionic layer adsorption and reaction (SILAR) method. The doping of lithium were studied for different at. wt. % in the $NiFe_2O_4$ thin film preparation. The thickness of Li doped $NiFe_2O_4$ thin films decreases as at. wt. % of Li increases in the Ni-Fe solution. XRD patterns revealed amorphous nature of thin films when at. wt. % of Li is increases and undoped thin film shows crystalline nature. Surface morphological and wettability properties show as Li doping increases, the porosity and hydrophilic nature. This nature is suitable for supercapacitive application. The supercapacitive performance of lithium doped and undoped $NiFe_2O_4$ thin film electrodes was observed in various electrolytes and optimized in 1.0 M Na_2SO_3 electrolyte. The maximum specific capacitance of 449 F/g was obtained for optimized 3 at.wt. % Li doped $NiFe_2O_4$ electrode.

Keywords: Thin films; Li doped $NiFe_2O_4$; SILAR; Supercapacitors; SEM

***Corresponding authors email id:** vinayakjamadade@gmail.com

1 Introduction

Electrochemical capacitors have the potential to emerge as a promising energy storage devices. As a consequence, many research efforts are focused on designing new materials to improve energy and power densities. There are various materials used for supercapacitor application such as Ag/Au/Polypyrrole [1], Co_3O_4/N-CP [2], CuO [3], NF/G/V_2O_5 [4], RuO_2/Fe_2O_3 [5], etc.

From literature survey lithium doping shows enhance supercapacitive performance of electrodes [6]. $NiFe_2O_4$ nanoparticles have typical ferromagnetic properties, low conductivity, low eddy current losses, high electrochemical stability, catalytic behaviour and abundance in nature. It is used in information storage, spintronics, magnetic resonance imaging, microwave devices, suitable electrodes for Li-ion batteries and supercapacitors [7-8]. G. Dixit et al. [9] studied the effect of Ce doping on magnetic properties of $NiFe_2O_4$. Recently researches are attracted towards Li-$NiFe_2O_4$ thin films for supercapacitor devices due to its simplicity, low-cost, good electrochemical performance, and more cyclic stability [10]. For preparation of $NiFe_2O_4$ thin films, various physical and chemical methods are used. The physical methods have many drawbacks such as a small area of deposition, requirement of sophisticated instruments, cost of a system, wastage of depositing material etc. There are various chemical methods used for preparation for $NiFe_2O_4$ thin films such hydrothermal [11], auto-combustion [12], thermal hydrolysis [13], spray pyrolysis [14], electrodeposition [15] etc. Recently, Gunjakar et al. [16] reported nanocrystalline $NiFe_2O_4$ thin films obtained from CBD method. In the present we are using cost-effective SILAR method. The purpose of this research work is to enhancement of stable ferrite material for supercapacitor

application by simple SILAR method that has the great advantage due to low cost for commercial application [17]. In the present work Li-$NiFe_2O_4$, thin films with different doping percentage of Li have been synthesis on stainless steel substrates using SILAR method. As per the literature survey, there is no report for synthesis of Li doped $NiFe_2O_4$ thin films using SILAR method for supercapacitor. The thickness, structural, morphological and wetabilitical properties of Li doped and undoped $NiFe_2O_4$ thin films were studied. Also supercapacitive performance of SILAR deposited Li-doped / undoped $NiFe_2O_4$ thin films have been studied successfully.

2 Experimental

2.1 Characterizations

The thickness Li doped and undoped $NiFe_2O_4$ of thin films was measured by gravimetric weight difference method using sensitive microbalance. The structural properties of thin films were determined using X-ray diffraction (XRD) technique using Philips (PW-3710) diffractometer model with the chromium target (λ= 2.28 Å) in the range of 20-80^o. The surface morphology of thin films was observed by using scanning electron microscopy (SEM) of model JEOL-6360. The wetabilitical studies were carried out by Rame-hart USA equipment with CCD camera. The cyclic voltammetry (CV) experiments were performed using potentiostat/galvanostat (EG & G PAR 263-A) to determine the specific capacitance.

2.2 Preparation of Li doped and undoped-$NiFe_2O_4$ thin films

Li doped and undoped-$NiFe_2O_4$ thin films were deposited onto stainless steel substrates using SILAR method. Synthesis of Li doped and undoped $NiFe_2O_4$ films was

carried out onto previously cleaned stainless steel substrates by alternate immersion of the substrate in cationic precursor $NiCl_2$, $FeCl_2$ i. e. (Ni^{+2}, Fe^{+2}) source kept at 333 K and anionic precursor as double distilled water, kept at 300 K [18]. Aqueous combined nickel (II) chloride and iron (II) chloride solution used as a source of Ni^{+2} and Fe^{+2} ions, was made alkaline pH 9.2 adjusted by ammonia solution source of oxygen ions and the complexing agent. Concentration ratios of the Ni^{+2} and Fe^{+2} were kept fixed as 0.1 M: 0.2 M, i. e. 1:2. First, the ultrasonically cleaned stainless steel substrate was immersed in combined alkaline nickel chloride and iron chloride solution so as to get nickel and iron hydroxides adsorbed onto the substrate. Afterwards, the substrate was rinsed with double distilled water kept at 300 K where the oxygen ions reacted with pre-adsorbed nickel and/or iron hydroxide on the stainless steel substrates. These films are drying by hot air after each cycle and annealed at 723K for 3h to form $NiFe_2O_4$ films.

3 Results and discussion

3.1 Thickness measurement

Fig. 1 shows the variation of $NiFe_2O_4$ film thickness with a number of deposition cycles. The film thickness increased with deposition cycles from 0 to 70. Further, $NiFe_2O_4$ film thickness decreased due to the formation of the outer porous layer as the film started peeling off from the substrate. The optimized $NiFe_2O_4$ film has a maximum terminal thickness of $NiFe_2O_4$ film is about 1.40 µm. Such $NiFe_2O_4$ films are used for further characterization. Similarly $NiFe_2O_4$ films prepared with Li doping at 1 at. wt. %, 2 at. wt. %, and 3 at. wt. % of Li-$NiFe_2O_4$ thin films show the 1.30, 1.24, and 1.20 µm thickness respectively. In addition the thickness of films changes with Li doping. Z. Hai et al. [18]

reported as the thickness of materials reduces the specific capacitance of materials are improved.

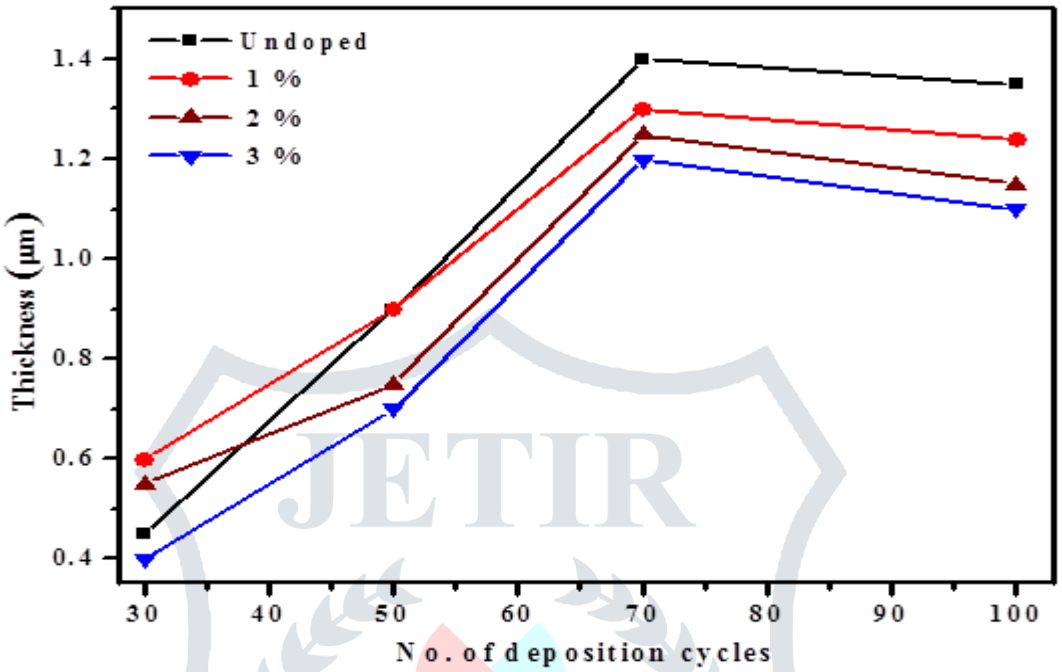

Fig. 1. Variation of doped and undoped $NiFe_2O_4$ film thickness at different doping concentration of Li.

3.2 XRD measurement

XRD patterns of undoped and Li doped annealed $NiFe_2O_4$ films are shown in Fig. 2. The crystal structure of prepared $NiFe_2O_4$ is confirmed with JCPDS card no. 74-2081. The peaks of stainless steel substrates are marked by triangle (Δ). The orientations corresponding to (220), (311), and (400) planes. The (311) peak shows high intensity for $NiFe_2O_4$ film and after Li doping in $NiFe_2O_4$ the intensive peak is found at (400). As at. wt. % of Li doping is increased in the NiFe bath, the crystallinity of $NiFe_2O_4$ films is decreased. Due to this reason, the (220) and (311) peaks are not found in Li doped $NiFe_2O_4$ thin films. The small peak intensities in XRD pattern revealed the existence of fine grains with most of the part as

amorphous. The Table 1 shows the 2θ °, hkl planes, observed and standard 'd' values of undoped $NiFe_2O_4$ thin films.

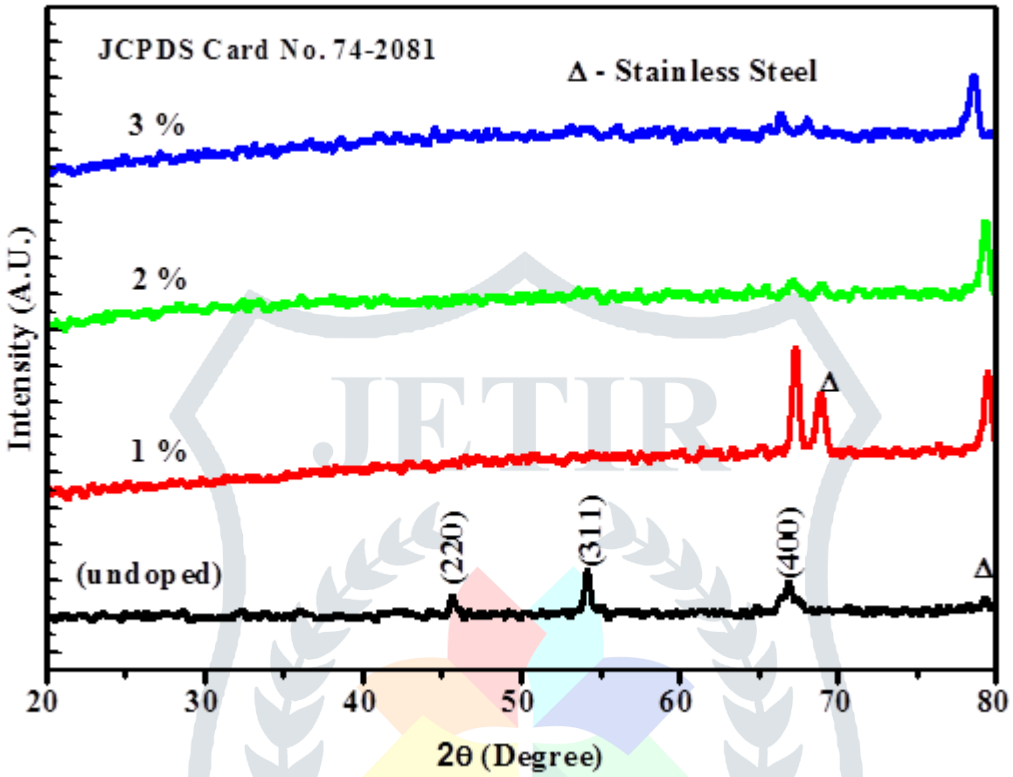

Fig. 2. XRD patterns of Li doped and undoped $NiFe_2O_4$ thin films onto stainless substrates.

Sr. No.	2θ °	hkl planes	Observed 'd' values	Standard 'd' values
1	45.63	220	2.9510	2.9478
2	54.20	311	2.5166	2.5139
3	66.74	400	2.0890	2.0844

Table 1. 2θ °, hkl planes, observed and standard 'd' values of undoped $NiFe_2O_4$ thin films.

Crystallite size (D) of doped and undoped $NiFe_2O_4$ was determined using the well-known Debye Scherrer's equation [19]:

$$D=0.9\lambda/\beta\cos\theta \quad (1)$$

Where θ is the Bragg's angle, D is crystallite size, β is full width at half maximum of the peak in radian, λ is the wavelength of X-ray used, and 0.9 is a constant. The crystallite size (D) was observed for highest intensity diffraction peak (311) of undoped $NiFe_2O_4$ and we found 35 nm. It shows that the nanocrystalline films are formed.

3.3 Surface morphological studies

The surface morphological studies of the undoped and Li doped $NiFe_2O_4$ films have been carried out by scanning electron micrograph. SEM images of X 10,000 magnification and are shown in Fig. 3 (a, b, c, and d), respectively.

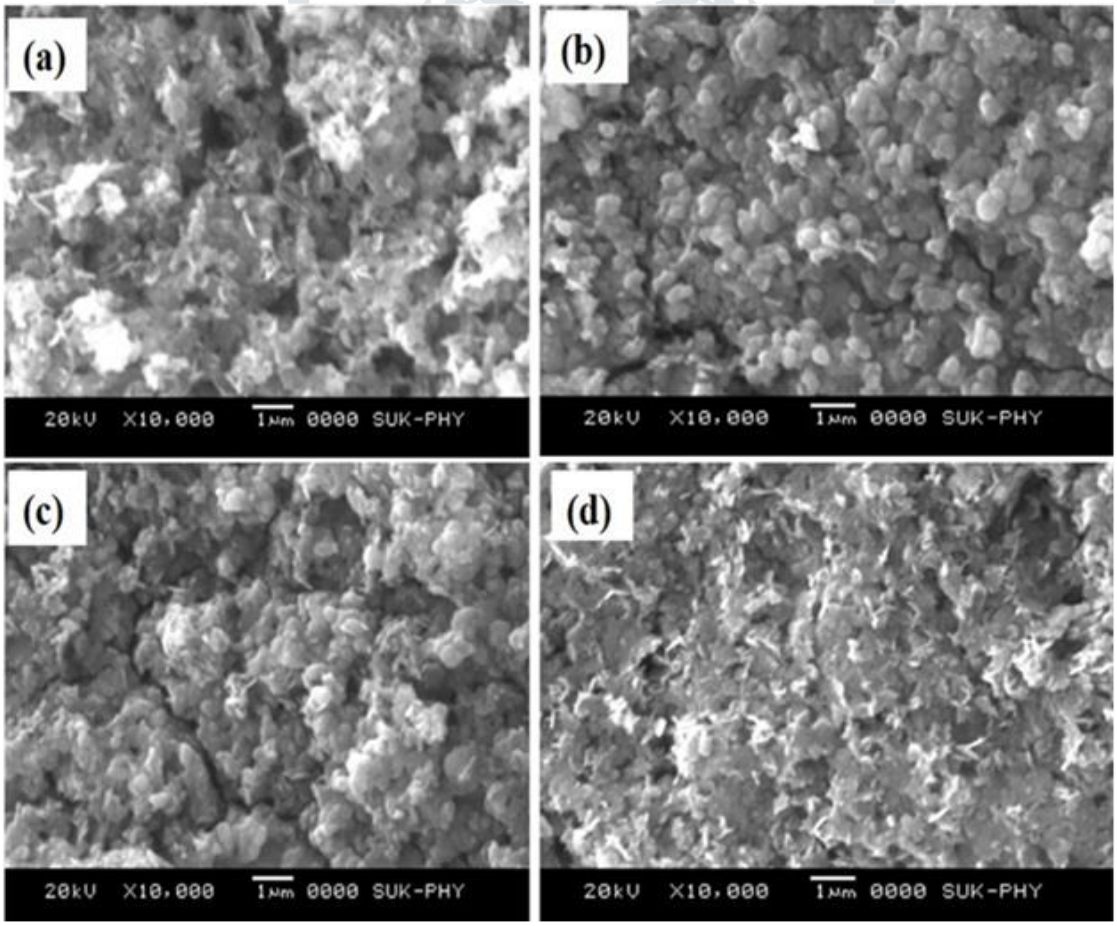

Fig. 3. SEM images of (a) $NiFe_2O_4$, (b) 1 at. wt. %, (c) 2 at. wt. %, and (d) 3 at. wt. % Li doping of $NiFe_2O_4$ films at X10,000 magnifications.

The micrograph of $NiFe_2O_4$ thin film shows flake like structure which is randomly grown on the substrates. Fig. 3 (b, c, and d) of Li doped $NiFe_2O_4$ shows granular grain like morphology for 1 at. wt. %, 2 at. wt. %, and 3 at. wt. % respectively. The doping concentration of Li in bath increases as the the particle size and surface was changed [20]. J. A. Lee et al. [21] reported an effect of Li doping on duplex microstructures of thin films show second phases in the inner region of films. It shows that the morphology of films changes with doping percentage of Li. It is useful for supercapacitor applications.

3.4 Wettability measurement

Fig. 4 (a, b, c, d) shows that water contact angle measurement images of Li undoped-doped $NiFe_2O_4$thin films at different at. wt. % of Li doping.

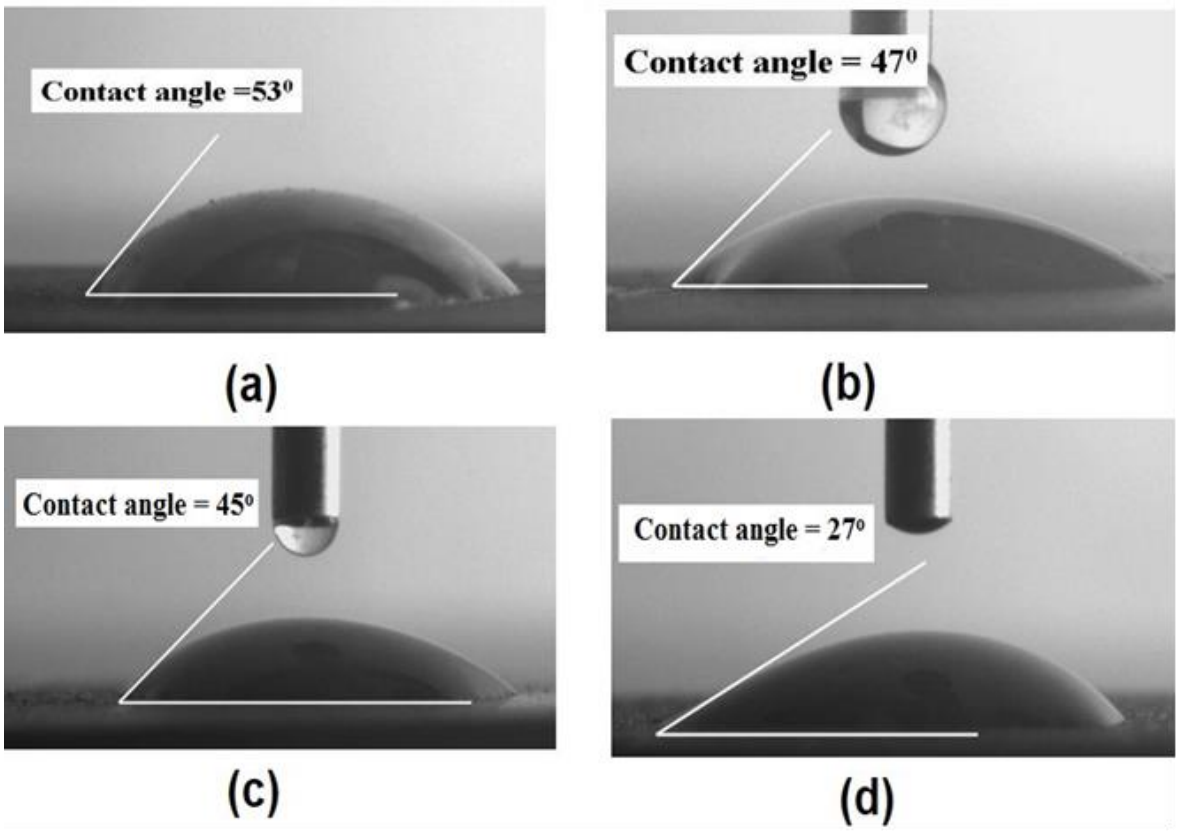

Fig. 4. Contact angle images of (a) $NiFe_2O_4$, (b) 1 at. wt. %, (c) 2 at. wt. %, and (d) 3 at. wt. % Li doping of $NiFe_2O_4$ films surfaces which is deposited onto stainless steel substrates.

The observed water contact angles for (a) $NiFe_2O_4$, (b) 1 at. wt. % Li doped, (c) 2 at. wt. %, and (d) 3% at. wt. Li doped films on stainless steel substrates are 53º, 47º, 45º, and 27º respectively. It reveals that the hydrophilicity of $NiFe_2O_4$ films are increases with doping of Li. Hence, water contact angle depends not only on the preparation method but also depends on the doping concentration. The hydrophilic nature of the surface is necessary for better supercapacitive performance [22]. Also due to change in surface morphology the contact angle of thin films decreased from 53º to 27º and the lower contact angle is may be better for improvement in supercapacitive performance [23].

3.5 Supercapacitor studies of Li doped and undoped $NiFe_2O_4$ thin film electrode

The supercapacitive studies were carried out in a three-electrode electrochemical cell, in which the Li-$NiFe_2O_4$ thin film as working electrode, platinum as the counter, and saturated calomel electrode (SCE) as the reference electrode. The cyclic voltammogram (CV) of doped and undoped $NiFe_2O_4$ thin film electrode with 0 to 1 V potential at scan rate 10 mV/s in optimized and suitable 1 M Na_2SO_3 electrolyte. The 1 M Na_2SO_3 electrolyte was chosen which was able to give maximum capacitance as compare to other electrolytes for Li doped and undoped $NiFe_2O_4$ film electrodes. The typical cyclic voltamograms (CV) in Fig. 5 (A) show SILAR deposited undoped, 1 at. wt. %, 2 at. wt. %, and 3 at. wt. % Li doped $NiFe_2O_4$ films at the scan rate of 10 mV/s.

The supercapacitor performance of SILAR deposited Li doped and undoped $NiFe_2O_4$ film electrodes were carried out in the 1 M Na_2SO_3 electrolyte. The effect of at. wt. % of Li doping on supercapacitor performance of films are revealed that as the Li doping increased from (a) undoped, (b) 1 at. wt. %, (C) 2 at.wt. %, (d) 3 at.wt. %. As the current under the curve is increased the specific capacitance of films are increased from 200 to 449 F/g. The

maximum specific capacitance of 449 F/g is obtained for 3 at.wt. % Li doped $NiFe_2O_4$ film electrode at the scan rate of 10 mV/s. While if there is only $NiFe_2O_4$ electrode without doping shows less specific capacitance [24]. It means that Li doping in $NiFe_2O_4$ thin films increases the specific capacitance of films.

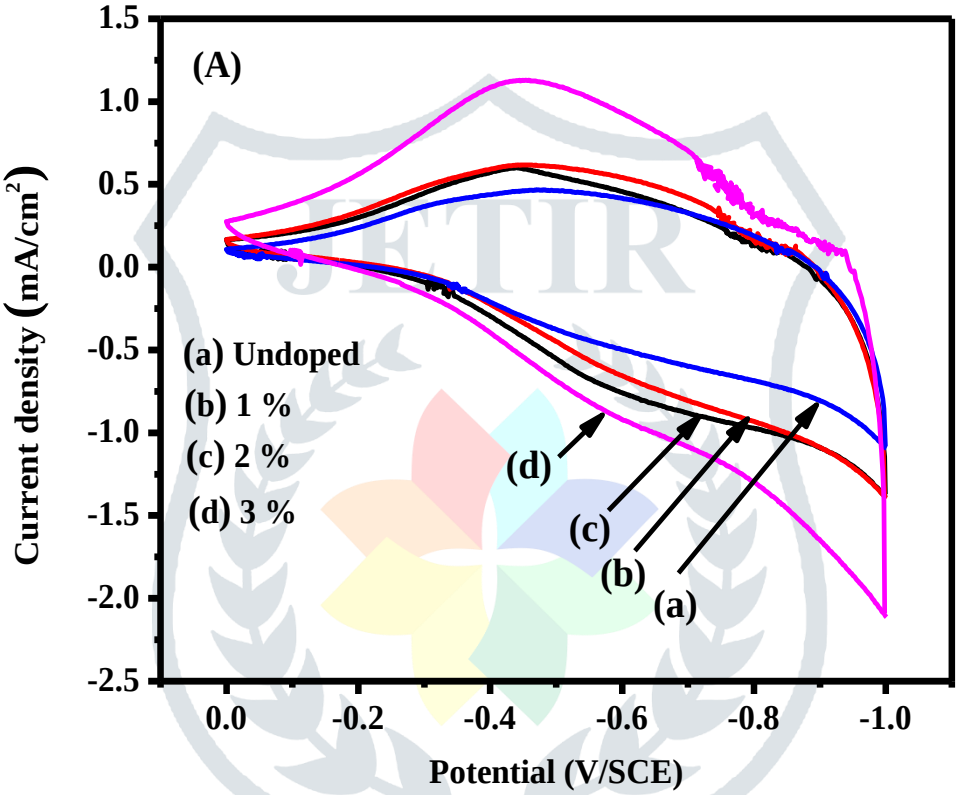

Fig. 5 (A) Cyclic voltamograms (CV) effect of; (a) undoped, (b) 1 at.wt. %, (C) 2 at.wt. %, (d) 3 at.wt. % Li doping $NiFe_2O_4$ films at the scan rate of 10 mV/s.

In Fig. 5 (B) as a specific capacitance of $NiFe_2O_4$ thin films increases with doping % of lithium. The specific capacitance of undoped $NiFe_2O_4$ thin films is found to be 200 F/g while for 1 at.wt. %, 2 at.wt. %, 3 at.wt. % of Li doping $NiFe_2O_4$ films are 323, 379, 449 F/g respectively.

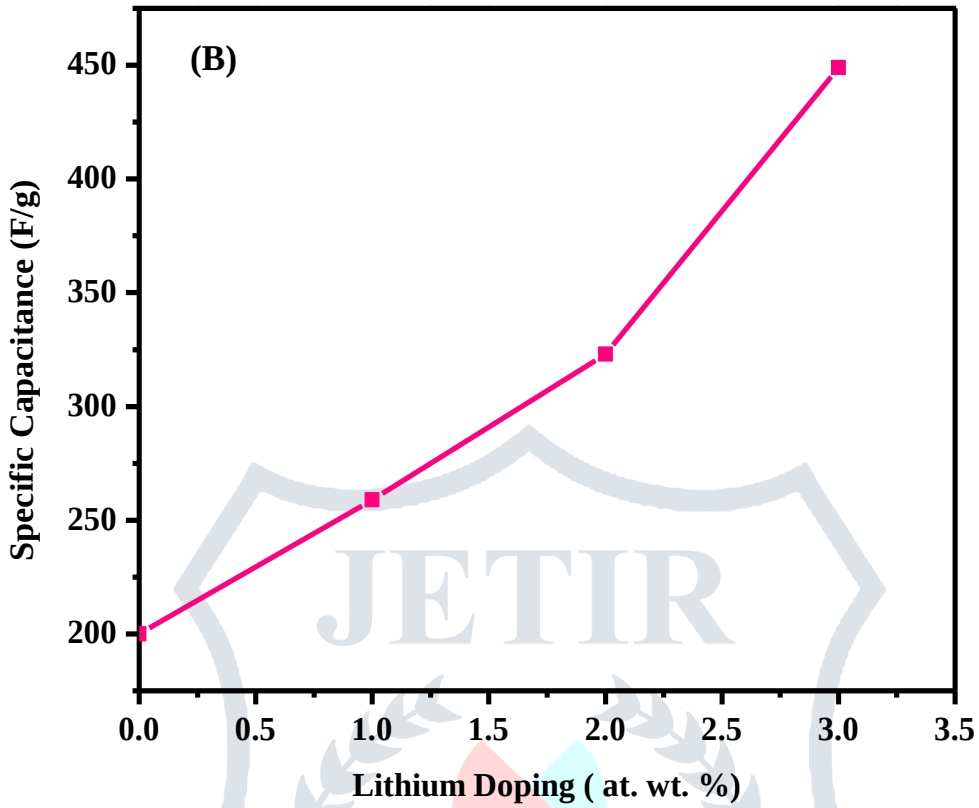

Fig. 5 (B) Effect of; (a) undoped, (b) 1 at.wt. %, (C) 2 at.wt. %, (d) 3 at.wt. % Li doping on specific capacitance of $NiFe_2O_4$ films.

Sr. No.	At. wt. % of Li	Specific capacitance (F/g)
1	0	200
2	1	323
3	2	379
4	3	449

Table 2. At. wt. % of Li doping and specific capacitance of $NiFe_2O_4$ thin films.

Table 2 shows doping percentage Li in $NiFe_2O_4$ and specific capacitance films. The lithium atoms enhance an electrocatalytic activity inside the $NiFe_2O_4$ thin films which results

in more specific capacitance after lithium doping [25]. Our result shows more specific capacitance due to increases in doping of Li atoms in thin films preparation.

4 Conclusions

In present work comparative study of Li doped and undoped $NiFe_2O_4$ thin films have been successfully studied using cost-effective SILAR method. The effect of 1 at. wt. %, 2 at. wt. %, and 3 at. wt. % of doped and undoped $NiFe_2O_4$ films onto their structural, morphological, thickness, contact angle and supercapacitive properties were studied. As the doping percentage increases the thickness of Li-$NiFe_2O_4$ thin films are decreases. The undoped films show crystalline nature of XRD and for Li doped $NiFe_2O_4$ films amorphous nature is observed. The lowest contact angle of Li-$NiFe_2O_4$ thin films is found to be 27^o for films deposited at 3 at.wt. % Li doping. The specific capacitance of Li-$NiFe_2O_4$ thin film electrodes increases with doping percentage of Li up to 3 at. wt. %. The maximum specific capacitance of 449 F/g was achieved for 3 at. wt. % Li-$NiFe_2O_4$ film electrode. Above all result shows the specific capacitance increases with doping percentage of Li in the $NiFe_2O_4$ thin film.

References

[1] H. Moon, H. Lee, J. Kwon, Y. D. Suh, D. K. Kim, I. Ha, J. Yeo, S. Hong, S. H. Ko, Sci. Rep. **7** (2017) 41981.

[2] Z. Lin, X. Qiao, Sci. Rep. 8 (2018) 1802.

[3] I. Y .Y. Bu, R. Huang, Ceramics International 43 (2017) 45.

[4] N. V. Hoa, T. T. H. Quyen, N. N. Huu, N. V. Hieu, J-J. Shim, J. Alloys Compd. 702 (2017) 693.

[5] D. Xiang, L. Yin, C. Wang, L. Zhang, Energy 106 (2016) 103.

[6] D. P. Dubal, D. Aradilla, G. Bidan, P. Gentile, T. J. S. Schubert, J. Wimberg, S. Sadki, P. Gomez-Romero, Sci. Rep. 5 (2015) 09771.

[7] M. I. Oshtrakh, M. V. Ushakov, B. Senthilkumar, R. K. Selvan, C. Sanjeeviraja, I. Felner, V. A. Semionkin, Hyperfine Interact 219 (2013) 7.

[8] X. Feng, Y. Huang, X. Chen, C. Wei, X. Zhang, M. Chen, J. Mater. Sci. 53 (2018) 2648.

[9] G. Dixit, P. Negi, J. P. Singh, R. C. Srivastava, H. M. Agrawal, J. Supercond. Nov. Magn. 26 (2013) 1015.

[10] H. Guo, T. Li, W. Chen, L. Liu, J. Qiao, J. Zhang, Sci. Rep. 5 (2015) 13310.

[11] D. K. Dinkar, B. Das, R. Gopalan, B. S. Dehiya, Mater. Chem. Phy. 218 (2018) 70.

[12] P. Sivakumar, R. Ramesh, A. Ramanand, S. Ponnusamy, C. Muthamizhchelvan, J. Mater. Sci. Mater. Electron. 23 (2012) 1011.

[13] T. S. Karpova, V. G. Vasil'ev, E. V. Vladimirova, A. P. Nosov, Inorg. Mater. Applied Res. 3 (2012) 107.

[14] J. Zheng, F. Song, S. Che, W. Li, Y. Ying, J. Yu, L. Qiao, Adv. Powder Tech. 29 (2018) 1474.

[15] P. D. Thanga, G. Rijnders, D. H. A. Blank, J. Mag. Magn. Mater. 310 (2007) 2621.

[16] J. L. Gunjakar, A. M. More, K. V. Gurav, C. D. Lokhande, Appl. Surf. Sci., 254 (2008) 5844.

[17] M. Rajesh, C. J. Raj, B. C. Kim, R. Manikandan, K. H. Kim, S. Y. Park, K. H.

Yu, Electrochim. Acta 240 (2017) 231.

[18] Z. Hai, M. K. Akbari, Z. Wei, C. Xue, H. Xu, J. Hu, S. Zhuiykov, Electrochim. Acta 246 (2017) 625.

[19] B. Shinde, S. Kamble, P. Gaikwad, V. Ghanwat, S. Tanpure, P. Pagare, B. Karale, A. Burungale, Res. Chem. Intermed. 44 (2018) 3097.

[20] D. P. Joseph, M. Saravanan, B. Muthuraaman, P. Renugambal, S. Sambasivam, S. P. Raja, P. Maruthamuthu, C. Venkateswaran, Nanotechnology 19 (2008) 485707.

[21] J.-A. Lee, H.-C. Lee, Y.-W. Heo, J.-H. Lee, J.-J. Kim, Ceramics International 42 (2016) 17339.

[22] V. S. Jamadade, V. J. Fulari, C. D. Lokhande, J. Alloys Compd. 509 (2011) 6257.

[23] V. V. Jadhav, M. K. Zate, S. Liu, M. Naushad, R. S. Mane, K. N. Hui, S.-H. Han, Appl. Nanosci. 6 (2016) 511.

[24] Y. Zhao, X. Le, J. Yan, W. Yan, C. Wu, J. Lian, Y. Huang, J. Bao, J. Qiu, L. Xu, Y. Xu, H. Xu, H. Li, J. Alloys Compd. 726 (2017) 608.

[25] J.-M. Li, K.-H. Chang, T.-H. Wu, C.-C. Hu, J. Power Sources 224 (2013) 59.